

CO₂ Solubility in Fast Pyrolysis Bio-oil

Clarissa Baehr, Ramazan Acar, Chaima Hamrita, Klaus Raffelt,* and Nicolaus Dahmen



Cite This: *Ind. Eng. Chem. Res.* 2023, 62, 15378–15385



Read Online

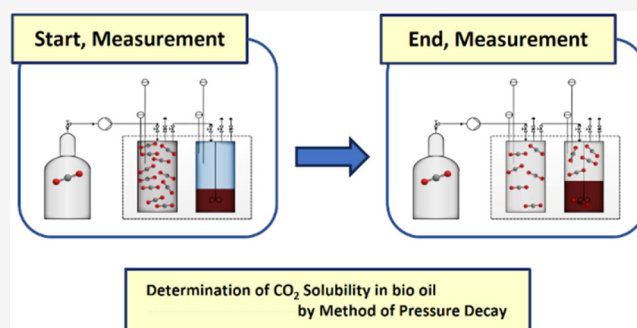
ACCESS |

Metrics & More

Article Recommendations

Supporting Information

ABSTRACT: Preheating and the use of additives, such as alcohols, are common strategies to treat fast pyrolysis bio-oil after production or before its intended use. Such strategies lower the viscosity of bio-oil and slow chemical reactions occurring in bio-oil during storage. Furthermore, they influence the physical-chemical properties, environmental performance, and cost of the final product. This work suggests the use of CO₂ as an alternative and environmental strategy. In contrast to other additives, CO₂ has the advantage of being a byproduct of the pyrolysis process. To assess CO₂ as an additive and solvent for bio-oil, solubility data on CO₂ in acetol, pure bio-oil, and mixtures of bio-oil with an added compound are provided. Experiments were conducted at 50 °C and pressures of 20–100 bar. As additional compounds, acetic acid, acetol, furfural, guaiacol, and water are deployed. The results showed that the CO₂ solubility is below 0.1 wt % at subcritical pressures but elevated at supercritical pressures. At 95 bar, the CO₂ solubility equates to 0.45 wt %. This is below the CO₂ solubility of butanol, which accounts for 0.6–0.7 wt % at the same pressure and is generally higher than the solubility in bio-oil. The CO₂ solubility in pure fast pyrolysis bio-oil and its mixtures can be well described by the SRK-EoS. This is a basis to draw a connection between the CO₂ solubility and its effects on the properties and further treatment.



1. INTRODUCTION

Fast pyrolysis bio-oil (FPBO) is commercially available as a burner fuel for industrial burners. This limits the application of FPBO as a source for heat production by combustion.^{1–3} The narrow scope of application is due to unfavorable properties. These include a high water content, high content of oxygenated organics, high acidity, high viscosity, and its ability to change the composition and physical-chemical properties when stored. The effect is often referred to as aging.^{3,4}

The aging phenomenon occurs due to the composition of FPBO consisting of more than 300 substances, with some being reactive. Those are pyrolytic lignin, phenols, sugar-type compounds, furfurals, acids, carbonyls, alcohols, and water.^{3,5–8} During aging, reactions with reactive components lead to molecules with an increased molar mass. This increases the average molar mass of FPBO, which, in turn, increases the viscosity. The changed polarity of the aging products can induce phase separation.⁹

The production of FPBO from renewable resources is possible via pyrolysis. The latter allows the conversion of various biological matrices containing cellulose, hemicellulose, and lignin to FPBO and to some amounts of pyrolytic gas and solids.¹⁰ The pyrolysis process takes place at a temperature of 500 °C with a low residence time of about 2 s. It is ended by rapid condensation to gain the liquid products, including some reactive substances and so leading to a thermodynamically unstable liquid mixture.^{11,12}

FPBO is produced commercially, inter alia, by Fortum (Finland),³ Envergent Technologies' RTP (Canada),¹³ and Twence/Empyro BV (Netherlands).¹⁴ As customary for other commercial fuels, with the use of FPBO as a burner fuel, its quality is defined by norms. These specify that FPBO must not exceed a certain viscosity and density, while setting other properties.^{1–3} A low and stable viscosity of FPBO is necessary, if pumped for transfer and atomized into a combustion chamber.³ To ensure the viscosity, the ASTM D7544–12¹ and EN 16900:2017² recommend preheating FPBO. Even though, this procedure requires energy and could cause or accelerate aging reactions because of elevated temperatures.¹⁵ Additionally, it is suggested to store FPBO under stirring and to use additives such as alcohols.^{1,2}

Alcohols reduce the viscosity due to dilution.¹⁶ This method also initiates esterification with organic acids common in FPBO, lowering their overall acidity.¹⁷ However, the addition of alcohols or preheating FPBO means additional costs if FPBO is chosen instead of conventional fuels. Substituting

Received: June 20, 2023

Revised: August 16, 2023

Accepted: August 22, 2023

Published: September 13, 2023



alcohols with a cheap and easily available solvent, which enhances further processing steps, can be an alternative.

Carbon oxides are abundant in pyrolytic gas, a byproduct of the pyrolysis process.^{10,12} In the context of extraction processes, for instance, CO₂ is already a well-known and commercially used solvent.^{18,19} Therefore, the question arises of whether or not CO₂ can be applied as a solvent to improve FPBO processing and handling. Possible beneficial improvements could be seen in the viscosity reduction for easier handling, resulting in less power consumption for pumping or filtration. Also, the presence of pressurized CO₂ could improve spray formation in nozzles during FPBO combustion and gasification processes by a reduced viscosity and additional expansion energy. Also, a higher hydrogen fraction in the liquid phase during hydro-treating of FPBOs for deoxygenation could be achieved, possibly resulting in a lower absolute hydrogen pressure of today up to 30 MPa, thus contributing to a significant process improvement.

However, it is not clear if CO₂ is soluble in FPBO and which pressures are necessary to establish solvation, since data on FPBO mixtures with CO₂²⁰ or others²¹ is scarce. Therefore, in the first place, this work intends to shed some light on the solubility of CO₂ in FPBO under conditions possible for short-term storage. The measuring temperature relates to a viscosity when FPBO is still transferable. It is an often-used reference temperature in such contexts.

The CO₂ solubility determination is realized by lab-scale measurements conducted at 50 °C and pressures of 20–100 bar. The solubility in acetol, pure FPBO, and mixtures with FPBO containing one model compound was determined. Furthermore, the Soave–Redlich–Kwong equation of state (SRK-EoS) was fitted to the CO₂ solubility in pure FPBO. With these fitting parameters, mixtures composed of FPBO and a model compound could be described. On a more general note, the characteristics of the solubility behavior of CO₂ in FPBO are discussed, and possible advantages for the treatment of FPBO with CO₂ are addressed.

2. MATERIALS AND METHODS

2.1. FPBO and Chemicals. The used FPBO was produced by the bioliq pilot plant. This plant is part of the bioliq-process operated at the Karlsruhe Institute of Technology. It is described elsewhere.^{22,23} As biomass, miscanthus was deployed. The pyrolysis was conducted at 500–600 °C and the condensation at 80–90 °C. The feed rate amounts to 500 kg h⁻¹.

Carbon dioxide (99.995%, CAS RN 124–38–9) is provided by Air Liquide. The model substances used are acetol (Alfa Aesar, 95%, CAS RN 116–09–6), acetic acid (Merck, ≥99%, CAS RN 64–19–7), furfural (Merck, ≥98%, CAS RN 98–01–1), guaiacol (Acros Organics, ≥99%, CAS RN 90–05–1), and purified water. The validation is carried out with *n*-butanol (Merck, ≥99%, CAS RN 71–36–3).

2.2. Experimental Setup and Measurement Procedure. *CO₂ Solubility.* The CO₂ solubility is determined by a static, synthetic method, which is known as the pressure-decay method.^{24,25} Here, the solved amount of CO₂ is calculated by a CO₂ mass balance, which results from the pressure drop in the gas reservoir at constant temperature, when the CO₂ expands into a second vessel, which contains the liquid. In doing so, the experimental setup shown in Figure 1 is used. It is similar to other setups conducting isothermal *p*-*T*-*x* measurements for determining the solubility or diffusion coefficient in liquids,

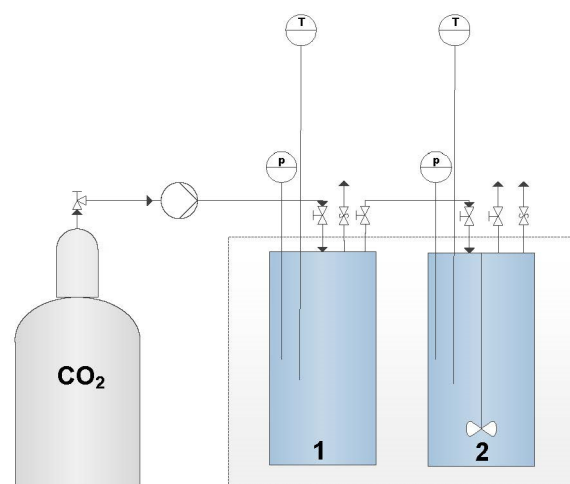


Figure 1. Experimental setup for solubility determination with gas reservoir (1) and equilibrium cell (2).

either by pressure drop or other ways to determine the fluid amount.^{24,26–28} The gas reservoir holds 0.320 L, and the equilibrium cell holds 0.210 L. The stated volumes consider the volumes of the attachments of the vessels. Each vessel is respectively equipped with a thermometer and a pressure sensor (Keller Druckmesstechnik, PA-33X/80794, $p_{\max} = 300$ bar) and the equilibrium cell with a stirrer (Premex Solutions GmbH, PRE 1898 04.17 90 N cm), additionally. During the measurement, the temperature and pressure are controlled and recorded continuously using the software HITEC Zang GmbH, Labvision (version 2.11.1.0). The gas reservoir is filled by a syringe pump (ISCO, Syringe pump Model 500D) with CO₂. The vessels are heated in an aluminum block. A ceramic mat and vermiculite plates provide insulation. In order to minimize heat losses on the surface as well, the upper part of the vessels is insulated with BCTEX fleece material (Huckauf), which is individually adjusted for each experiment. The measurements are conducted at a temperature of 50 °C and a maximum pressure of about 100 bar.

The sample preparation and measurement procedure are as follows: The gas reservoir is equipped with CO₂, whose amount is known by pressure, temperature, and volume of the vessel using the Span–Wagner equation.²⁹ The second vessel is charged with the liquid. Its amount is known by the mass, which is 0.010–0.050 kg. The exact mass depends on the specifics of each particular experiment, such as the required time to reach a steady state and the absolute possible CO₂ amount solved. The calibration with water is conducted with 0.100 kg. FPBO and other chemicals are used without any further processing. The model mixtures contain FPBO and one model substance. Mixtures with acetol are composed of the mass ratios 1:1, 1:3, and 1:7. Mixtures with acetic acid, furfural, and guaiacol follow the ratios 1:3 and 1:7. The mixture with water follows a ratio of 1:7.

The measurement system is purged, and the liquid is covered with CO₂ at ambient pressure. After heating the whole system, meaning both vessels, to 50.0 ± 0.1 °C, the experiment is started by connecting both vessels. CO₂ expands into the vessel with the liquid and is partly solved. When pressure is stable (±0.1 bar) and the temperature equals the starting temperature (±0.1 °C), a steady state is reached. This procedure results in a pressure drop in the gas reservoir, which is related to the solubility.

The calculation of the CO₂ is conducted on the basis of a CO₂ mass balance with $m_{0,R}$ being the CO₂ mass in the gas reservoir at the beginning and $m_{E,R}$ at the end in eq 1. Analogically, $m_{E,G}$ is the nonsolved CO₂ mass in the equilibrium cell at the end. The variable m_{CO_2} is the CO₂ mass solved, and m_C is a correction term, which depends on pressure, temperature, and the individual device. Since the temperature and device are constant, m_C is only pressure-dependent. It can be derived by measurements with a reference substance. Here, it is done with water (calibration).

$$m_{0,R} = m_{E,R} + m_{E,G} + m_{CO_2} + m_C(p) \quad (1)$$

The CO₂ mass $m_{E,G}$ is given by the density at the end of the experiment $\rho_{CO_2,E}$ and the volume of the nonsolved CO₂. It is calculated by the volume V_G of the equilibrium cell and the volume of the liquid at the end $V_{L,E}$. A possible volume expansion of the liquid is considered using the density of the liquid $\rho_{L,E}$ and the mass of the liquid m_L . Then, eq 2 and eq 3 follow from eq 1. By substituting the CO₂ mass in the gas reservoir at the beginning $m_{0,R}$ and at the end $m_{E,R}$ by the product of the CO₂ density at the beginning $\rho_{CO_2,0}$, respectively, the end $\rho_{CO_2,E}$ and the volume of the gas reservoir V_R in combination with rearranging eq 3, the term for calculating the solved CO₂ mass m_{CO_2} is obtained in eq 4.

$$\rho_{CO_2,0} \cdot V_R = \rho_{CO_2,E} \cdot V_R + \rho_{CO_2,E} \cdot (V_G - V_{L,E}) + m_{CO_2} + m_C \quad (2)$$

$$m_{0,R} = m_{E,R} + \rho_{CO_2,E} \cdot \left(V_G - \frac{m_{CO_2} + m_L}{\rho_{L,E}} \right) + m_{CO_2} + m_C \quad (3)$$

$$m_{CO_2} = \frac{\rho_{CO_2,0} V_R + \rho_{CO_2,E} \cdot \left(-V_R - V_G + \frac{m_L}{\rho_{L,E}} \right) - m_C}{1 - \frac{\rho_{CO_2,E}}{\rho_{L,E}}} \quad (4)$$

2.3. Density of CO₂ Saturated Liquid. To identify a significant volume expansion of the liquid, which might occur during the solubility experiment, the density of the saturated CO₂ liquid is determined. It is measured by a density sensor (Emerson, FDM Fork Density Meter) attached into an autoclave with a volume of 2.000 L. The CO₂ is transferred by a syringe pump (ISCO, syringe pump Model 500D). The pressure, temperature, and density are measured and recorded throughout the experiment by the software ProLink III Basic. It allows control of the temperature as well. The experiments are conducted at the same temperature and pressure conditions as the solubility determination. Furthermore, a steady state at the beginning of every pressure step is presupposed, which means stable pressure and a stable temperature at 50 °C.

2.4. Simulation of CO₂ Solubility. The CO₂ solubility in FPBO and the mixtures are described by the Soave–Redlich–Kwong equation of state (SRK-EoS).³⁰ Theoretically, this requires certain parameters such as critical data and acentric factors, which are not met by all components in FPBO. Because of its complex composition, it is arguable to describe FPBO by simple model mixtures. Here, it is treated as a pseudo-single substance, which possesses critical data (critical pressure p_c , critical temperature T_c , critical volume V_c), a boiling point T_b , a uniform molar mass M , density ϑ , and

acentric factor ω . Connected to these parameters are also the molar volume, V_M and the molar amounts, x_i and x_j .

To achieve that, a theoretical surrogate for FPBO is created with partly hypothetical properties, which are gained by fitting the experimental results of FPBO. In turn, this surrogate for FPBO is applied to the description of the model mixtures. The mixtures are represented by combining the surrogate FPBO with a respective model substance, taking into account the mass ratios of the experiment. Van-der-Waals mixing rules are used and the mixing parameter k_{ij} is set to 0.^{30–32} The simulation is conducted by mixing the liquid with an excess of CO₂ with the program Aspen HYSYS V12.³³ It is processed by a separator.

$$p = \frac{RT}{V_M - b} - \frac{a}{V_M(V_M + b)} \quad (5)$$

$$a = 0.42748\alpha \cdot \frac{R^2 T_c^2}{p_c} \quad (6)$$

$$b = 0.08664 \cdot \frac{RT_c}{p_c} \quad (7)$$

$$\alpha = \left(1 + \kappa \left(1 - \left(\frac{T}{T_c} \right)^{0.5} \right) \right)^2 \quad (8)$$

$$\kappa = 0.48 + 1.574\omega + 0.176\omega^2 \quad (9)$$

$$a = \sum_i \sum_j (x_i x_j \cdot (a_i a_j)^{0.5} \cdot (1 - k_{ij})) \quad (10)$$

$$b = \sum_i (x_i b_i) \quad (11)$$

3. RESULTS AND DISCUSSION

3.1. Validation of the Experimental Setup. The experimental setup for the CO₂ solubility determination is validated by a system of CO₂/*n*-butanol at 50 °C, since *n*-butanol has a high CO₂ solubility. To correct systematic errors, a calibration with water is conducted. Contrarily to *n*-butanol, water has a very low CO₂ solubility. Thus, the applicability of the measurement system is ensured for liquids with high and low CO₂ solubilities at pressures of 20–100 bar.

For the calibration with water, the data from Briones *et al.*,³⁴ Bamberger *et al.*,³⁵ and Lucile *et al.*³⁶ at 20–100 bar are averaged by the exponential approach in eq 12, which leads to a pressure-dependent correction summand m_C for the CO₂ balance. For the validation with *n*-butanol, the data from Yun and M. R. Shi,³⁷ Lim *et al.*,³⁸ and Kariznovi *et al.*³⁹ are used as references. The CO₂ solubility in *n*-butanol was calculated by using the literature values of Zúñiga-Moreno *et al.*⁴⁰

$$x_{CO_2}(p) = l + m \cdot \exp(np) \quad (12)$$

The comparison of the experimental values for *n*-butanol with data is displayed in Figure 2 as mass fraction w_{CO_2} . It reveals the agreement between the values, especially for pressures above 90 bar and pressures below 60 bar. Around the critical pressure, the experiments lead to slightly higher values with a deviation of around 10%.

The density measurement is calibrated with water at 20 and 50 °C. The measurement ability is verified by the measurement

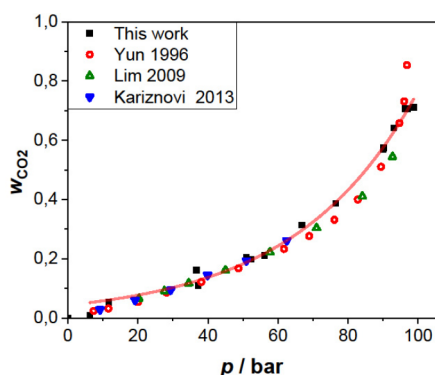


Figure 2. Comparison of experimental values for the CO₂ solubility in *n*-butanol as mass fraction w_{CO_2} .

of previously characterized FPBO. The error deviation equates to 60 kg m⁻³ (2 standard deviations).

3.2. CO₂ Solubility in Pure Liquids and Corresponding Density. Besides *n*-butanol, the CO₂ solubility in acetol and FPBO was determined. For acetol, there is a continuous increase of the solubility with the pressure, starting from $w_{\text{CO}_2} = 0.1$ at 23 bar, whereas the CO₂ solubility in FPBO exhibits a substantially lower solubility at pressures below the supercritical pressure of CO₂. At pressures between 75 and 95 bar, the solubility increases sharply for FPBO. Then, the CO₂ solubility in FPBO and in acetol are similar. The evolution of the CO₂ solubility in both substances dependent on the pressure is depicted in Figure 3.

This solubility behavior of FPBO can be modeled by the SRK-EoS, if FPBO is treated as a pseudo single substance with certain properties assigned to it, including hypothetical properties. They are summarized in Table 1. Density is taken as known from the literature.⁴¹ It fits to the here conducted density measurements. The normal boiling point is similar to substituted phenols such as guaiacol, a usual composite of FPBO. The molar mass lies in the region of pyrolytic lignin. The order of this property is essentially necessary to model the solubility behavior concerning the pressure dependence. The critical data T_c and p_c are in the size of substituted phenols, from which V_c follows. The acentric factor is chosen in plausible limits.

As the illustration of the experimental and simulated results in Figure 3b shows, the solubility by the model for FPBO

Table 1. Parameters to Define FPBO and CO₂ by SRK-EoS

parameter	FPBO	CO ₂
molar mass/g mol ⁻¹	2150	44.01
normal boiling point/°C	200	-78.6
density/kg m ⁻³	1200	825.3
T_c /°C	550	31.0
p_c /bar	17.05	73.7
V_c /m ³ kmol ⁻¹	0.3229	0.0939
acentric factor	0.1000	0.2389

aligns well. It is apparent that the FPBO solubility was determined at least three times for five approximately equidistant pressures between 20 and 100 bar. This indicates a measurement uncertainty dependent on the pressure. It is quantified by the standard deviation of each pressure step. It is in the range of 6–27% at most pressure stages. At the stage of 41 bar, the error equates to 41%.

For the density of the FPBO, no significant pressure dependency can be measured. This implies that no significant volume expansion of FPBO takes place during the solvation process, which could influence the CO₂ solubility determination considerably. The density of FPBO is 1150–1200 kg m⁻³ and for acetol is 1050–1060 kg m⁻³.

3.3. CO₂ Solubility in FPBO Mixtures. The measurement procedure for the mixtures with FPBO is conducted as in the previous experiments. The mixtures were prepared with FPBO and one model substance, which was acetol, acetic acid, furfural, guaiacol, and water. The densities of these mixtures are similar to pure FPBO, and no volume expansion could be observed. Therefore, the calculation of the CO₂ solubility is conducted with the density of FPBO.

The CO₂ solubility in the FPBO mixtures with acetol is shown in Figure 4a–c. In all mixtures, the CO₂ solubility is higher than in pure FPBO, while the solubility in the mixture with 12.5 wt % acetol is the lowest. Every data set of a mixture is fitted exponentially by eq 12, because the fit is hardly susceptible to single outliers, which makes it more suitable for comparison to other data sets. The single values of all measurements are summarized in the supplement.

At lower pressures, a slight increase of the solubility due to the acetol concentration can be recognized compared to pure FPBO. The curve shape of the fits to the solubility of the acetol mixtures is more similar to acetol in regard to the curvature. In general, the mixtures behave more like pure acetol. At higher

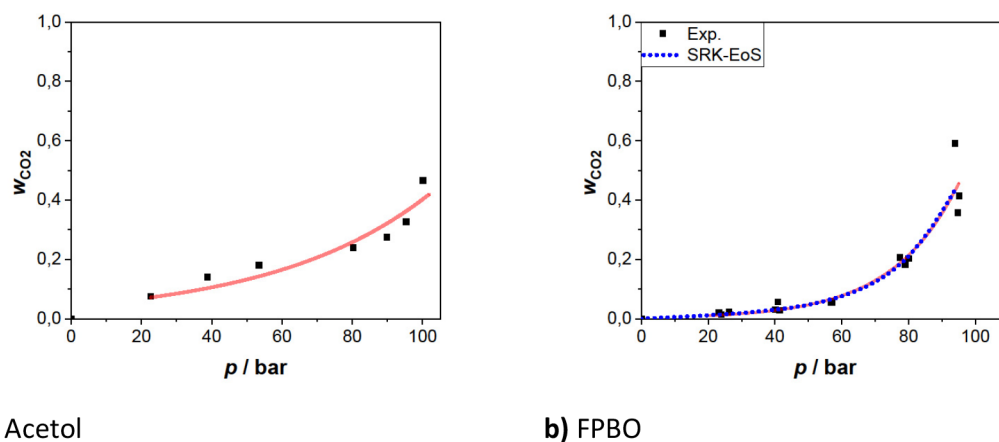


Figure 3. CO₂ solubility in acetol and FPBO at 50 °C.

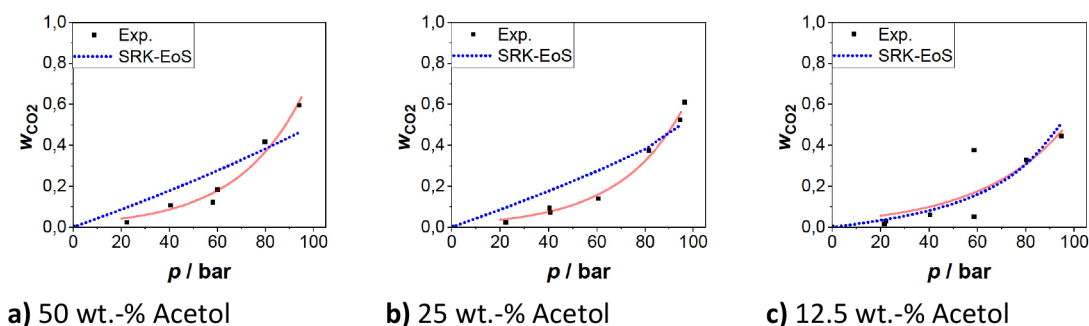


Figure 4. Comparison of the experimental results with the SRK-EoS for the CO₂ solubility in mixtures of FPBO and acetol at 50 °C.

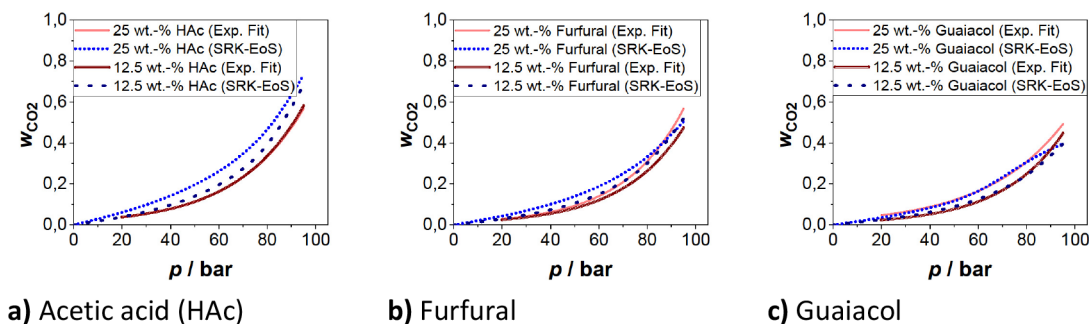


Figure 5. Comparison of the experimental results with the SRK-EoS for the CO₂ solubility in mixtures of FPBO and the model substances acetic acid, furfural, and guaiacol at 50 °C.

pressures of ca. 80–90 bar, this changes. From this point, there is a tendency of the CO₂ solubility to tend toward the CO₂ solubility in pure FPBO. The lower the acetol concentration, the lower is the CO₂ pressure, when this effect begins. This is probably due to a different solubility mechanism, whose influence depends on the applied pressure and organic fraction. In section 3.4, this behavior is discussed in more detail. The description by SRK-EoS works well for the mixture with 12.5 wt % acetol. For mixtures with 25 and 50 wt % acetol, the SRK-EoS gives higher values in the supercritical region. This is due to the linear increase in the solubility, originating from acetol as a component.

The CO₂ solubility for the other organic model substances resembles the data sets of acetol, principally, as seen in Figure 5. There is also a higher CO₂ solubility in the mixtures to observe compared to pure FPBO. At higher pressures, the CO₂ solubility tends toward the solubility in pure FPBO, as well. Also, the scattering is higher for mixtures with lower fractions of a model substance. Except the data sets for the mixtures with acetic acid, the solubility is higher, the higher the mass fraction of the respective model substance. Overall, the model substances acetic acid, furfural, and guaiacol lead to similar amounts of solved CO₂. The CO₂ solubility of all of these mixtures can be reproduced by the SRK-EoS. For the mixture with 25 wt % acetic acid, the theoretical solubility is somewhat higher. For all other data sets, the theoretical solubility is in good agreement with the experiments. This applies particularly for the solubility below 85 bar. The deviation at pressures >85 bar, as seen for the simulation for the mixture with guaiacol, is probably due to the predicted solubility of FPBO into the CO₂ rich phase.

Contrarily to the organic model substances, the results for the water mixture show that the addition of water to FPBO hardly enhances the CO₂ solubility compared to pure FPBO as depicted in Figure 6. However, above the supercritical

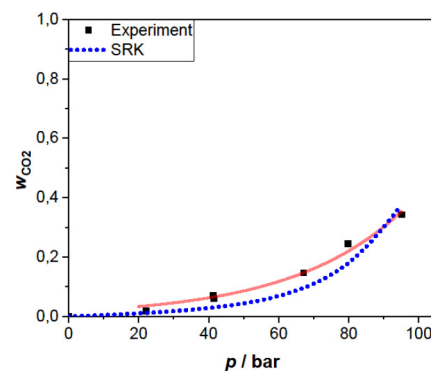


Figure 6. Comparison of the experimental results with the SRK-EoS for the CO₂ solubility in mixtures of 87.5 wt % FPBO and 12.5 wt % water at 50 °C.

pressure, there is even a tendency that less CO₂ is solved. Here as well, the solubility can be described by the SRK-EoS. It is somewhat lower than the experimental data except for high pressures around 90–100 bar. This is probably due to the generally low solubility of water compared to FPBO brought into play by the parameters for SRK-EoS.

3.4. Reasons for the Solubility Behavior of FPBO.

FPBO has a pressure-dependent solubility behavior that is different from those of other pure substances. Most remarkable is the difference between the subcritical and supercritical region. FPBO diluted with model substances did not show this distinct behavior.

This behavior could be attributed to the composition of FPBO, which consists of water (25 wt %); small, organic molecules (30–50 wt %); and a fraction related to polymeric compounds such as pyrolytic lignin (15–25 wt %) and anhydro oligomers (20–30 wt %). The latter fractions are high-molecular and gained when lignin, hemicellulose, and

cellulose are broken down.^{5,42–44} Thus, FPBO is composed of molecules with very different molecular masses and polarities, which probably control the CO₂ solubility of FPBO.

Due to this peculiarity, FPBO can be viewed from two contrasting positions: FPBO can be considered as a mixture of rather small molecules, as it happens in model mixtures,^{45,46} or, alternatively, FPBO can be described by its high molecular weight components. Close to the last position are approaches used to explain the solubility in polymers.^{47–56}

In the case of small molecules, intermolecular forces determine the solubility. To solve CO₂, the solvent–solvent interactions must be broken first. Then, a stable CO₂–solvent interaction can be formed. A measure of the solvent–solvent interaction is the cohesion energy. The CO₂–solvent interaction can be estimated by ab initio calculations.⁵⁷ Therefore, the CO₂ solubility is favored in liquids with low interactions, which are similar to those of CO₂ by displaying C–O bonds. Therefore, CO₂ can act in the solution similarly to a molecule of FPBO.

To shed light on the CO₂ solubility in the pure model substances, the CO₂ solubility was calculated by SRK-EoS. The results are provided in Figure 7. As expected, the CO₂

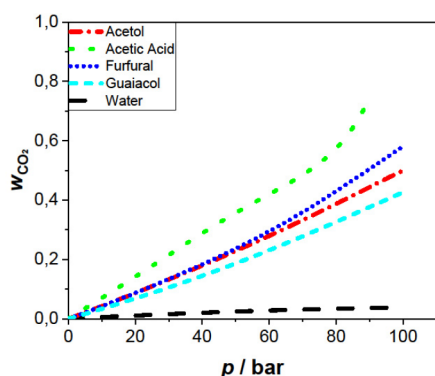


Figure 7. CO₂ solubility in the model substances acetol, acetic acid, furfural, guaiacol, and water by the SRK-EoS.

solubility is the lowest in water. In acetic acid, it is the highest. Both results can be confirmed by the literature.^{34–36,58} The other model substances, acetol, furfural, and guaiacol, possess a solubility that is in the same range and slightly below acetic acid.

At subcritical pressures, the CO₂ solubility in FPBO is like the solubility of water, which is plausible due to the high water content. In comparison to the CO₂ solubility in FPBO over the whole pressure range, as shown in Figure 3b, the solubility in the pure model substances behaves differently as it increases continually. No different gradient between the subcritical and supercritical regions can be observed for the theoretical values by SRK-EoS. This is similar for the measurements in pure *n*-butanol and acetol. Consequently, there are probably more factors in play for FPBO as for pure model substances in the supercritical region. These factors are mitigated if FPBO is diluted with another model substance as the measurements for the mixtures demonstrated.

This moves the focus to the polymeric fraction of FPBO. Regarding the CO₂ solubility in polymers, it is known that it is determined by solvent–solvent and CO₂–solvent interactions,^{59,60} but also by the free volume. This is known for the CO₂ solubility in products from heavy oil,^{47,48} ionic

liquids,^{49–52} or synthetic material.^{53–56} The factor of free volume relates to the unoccupied space in the liquid, in which CO₂ can be stored. As the CO₂ solubility in FPBO increases significantly above the critical pressure, the higher pressure probably facilitates the storage of CO₂ in vacancies. Possibly, the properties of supercritical CO₂ enhance the solubility additionally.

For FPBO mixtures, this effect is less pronounced because, at low pressures, the solubility is already increased due to the added model substance. At high pressures, starting around 80–90 bar, the solubility of the mixtures begins to converge to the solubility of pure FPBO. The point of convergence depends on the model substance added and its ratio in the mixture. Thus, the solubility of the mixture with 12.5 wt % water converges before 100 bar. If an organic model substance is used, especially with higher fractions, the necessary pressure for convergence is higher.

Therefore, it can be concluded that water limits the total amount of solved CO₂. This could be explained by two reasons: the generally low CO₂ solubility in water and its potential to fill vacancies in FPBO, because of its small size. Other substances do not show this effect as distinctly, owing to the fact that they are considerably larger than water, which might limit their ability to fill vacancies. Furthermore, the higher solubility of model substances other than water leads to an enhanced solubility in the mixture within a wider pressure range. Thus, the results point to two main factors, which determine the CO₂ solubility in FPBO: the concentration of low-molecular substances, mainly water, and the pyrolysis lignin fraction, which induces a solubility behavior common for polymers.

4. CONCLUSION

FPBO can solve significant amounts of CO₂, even though FPBO contains high amounts of water in combination with acid compounds. This is probably due to the high-molecular-weight organic fraction of FPBO. The CO₂ solubility is highly dependent on the pressure. At 50 °C and 95 bar, the CO₂ solubility in FPBO equates to 0.45 wt %. At 57 bar, the solubility is at 0.06 wt %. This indicates that, at low pressures, the solubility of FPBO is in the range of water. At higher pressures, the solubility is more comparable to acetol, which possesses a significant solubility. At 95 bar, acetol solves 0.3–0.4 wt % CO₂. Also at lower pressures, it has a high solubility. The difference of the CO₂ solubility in FPBO between sub- and supercritical pressures is unique for FPBO, when compared to the solubility in acetol, water, acetic acid, furfural, and guaiacol, which were used as model substances. Probably, at subcritical pressures, low-molecular compounds determine the CO₂ solubility, especially water, since the latter is the most abundant single component. At supercritical pressure, high-molecular-weight polymeric compounds such as the pyrolytic lignin fraction determine the CO₂ solubility with its free volume. CO₂ as a solvent for FPBO could be applied to dilute FPBO, in order to lower the viscosity and enhance usage in burners and for extracting valuable substances from FPBO.

■ ASSOCIATED CONTENT

Supporting Information

The Supporting Information is available free of charge at <https://pubs.acs.org/doi/10.1021/acs.iecr.3c02070>.

Tables with the measured values of the performed CO₂ solubility experiments (PDF)

AUTHOR INFORMATION

Corresponding Author

Klaus Raffelt – Institute of Catalysis Research and Technology, Karlsruhe Institute of Technology, 76344 Eggenstein-Leopoldshafen, Germany; orcid.org/0000-0001-5689-4443; Email: Klaus.Raffelt@kit.edu

Authors

Clarissa Baehr – Institute of Catalysis Research and Technology, Karlsruhe Institute of Technology, 76344 Eggenstein-Leopoldshafen, Germany

Ramazan Acar – Institute of Catalysis Research and Technology, Karlsruhe Institute of Technology, 76344 Eggenstein-Leopoldshafen, Germany

Chaima Hamrita – Institute of Catalysis Research and Technology, Karlsruhe Institute of Technology, 76344 Eggenstein-Leopoldshafen, Germany

Nicolaus Dahmen – Institute of Catalysis Research and Technology, Karlsruhe Institute of Technology, 76344 Eggenstein-Leopoldshafen, Germany

Complete contact information is available at:

<https://pubs.acs.org/10.1021/acs.iecr.3c02070>

Notes

The authors declare no competing financial interest.

REFERENCES

- (1) ASTM International. *ASTM D7544–12: Standard Specification for Pyrolysis Liquid Biofuel*; ASTM International, 2017.
- (2) DIN Deutsches Institut für Normung e.V. *DIN EN 16900:2017–05: Schnellpyrolyse-Biöle Für Industrielle Kesselanlagen - Anforderungen Und Prüfverfahren*; DIN Deutsches Institut für Normung e.V., 2017.
- (3) Oasmaa, A.; Van De Beld, B.; Saari, P.; Elliott, D. C.; Solantausta, Y. Norms, Standards, and Legislation for Fast Pyrolysis Bio-Oils from Lignocellulosic Biomass. *Energy Fuels* **2015**, *29* (4), 2471–2484.
- (4) Elliott, D. C.; Oasmaa, A.; Preto, F.; Meier, D.; Bridgwater, A. V. Results of the IEA Round Robin on Viscosity and Stability of Fast Pyrolysis Bio-Oils. *Energy Fuels* **2012**, *26* (6), 3769–3776.
- (5) Branca, C.; Di Blasi, C. Multistep Mechanism for the Devolatilization of Biomass Fast Pyrolysis Oils. *Ind. Eng. Chem. Res.* **2006**, *45*, 5891–5899.
- (6) Adhikari, S.; Nam, H.; Chakraborty, J. P. *Conversion of Solid Wastes to Fuels and Chemicals through Pyrolysis*; Elsevier B.V., 2018. DOI: [10.1016/B978-0-444-63992-9.00008-2](https://doi.org/10.1016/B978-0-444-63992-9.00008-2).
- (7) Staš, M.; Kubička, D.; Chudoba, J.; Pospíšil, M. Overview of Analytical Methods Used for Chemical Characterization of Pyrolysis Bio-Oil. *Energy Fuels* **2014**, *28* (1), 385–402.
- (8) Venderbosch, R. H.; Ardiyanti, A. R.; Wildschut, J.; Oasmaa, A.; Heeres, H. J. Stabilization of Biomass-Derived Pyrolysis Oils. *J. Chem. Technol. Biotechnol.* **2010**, *85* (5), 674–686.
- (9) Oasmaa, A.; Korhonen, J.; Kuoppala, E. An Approach for Stability Measurement of Wood-Based Fast Pyrolysis Bio-Oils. *Energy Fuels* **2011**, *25* (7), 3307–3313.
- (10) Yang, H.; Yan, R.; Chen, H.; Lee, D. H.; Zheng, C. Characteristics of Hemicellulose, Cellulose and Lignin Pyrolysis. *Fuel* **2007**, *86* (12–13), 1781–1788.
- (11) Alsbou, E.; Helleur, B. Accelerated Aging of Bio-Oil from Fast Pyrolysis of Hardwood. *Energy Fuels* **2014**, *28* (5), 3224–3235.
- (12) Bridgwater, A. V. Review of Fast Pyrolysis of Biomass and Product Upgrading. *Biomass and Bioenergy* **2012**, *38*, 68–94.
- (13) Envergent Technologies' RTP. <https://uop.honeywell.com/en/industry-solutions/renewable-fuels/rtp-biomass-conversion#> (accessed Aug 15, 2021).
- (14) Twence/Empyro BV. <https://www.btg-bioliquids.com/plant/empyro-hengelo> (accessed Aug 15, 2021).
- (15) Czernik, S.; Johnson, D. K.; Black, S. Stability of Wood Fast Pyrolysis Oil. *Biomass and Bioenergy* **1994**, *7* (1–6), 187–192.
- (16) Diebold, J. P.; Czernik, S. Additives To Lower and Stabilize the Viscosity of Pyrolysis Oils during Storage. *Energy Fuels* **1997**, *11*, 1081–1091.
- (17) Diebold, J. P. *A Review of the Chemical and Physical Mechanisms of the Storage Stability of Fast Pyrolysis Bio-Oils*; National Renewable Energy Laboratory: Golden, CO, 2000.
- (18) Cvjetko Bubalo, M.; Vidović, S.; Radojčić Redovniković, I.; Jokić, S. Green Solvents for Green Technologies. *J. Chem. Technol. Biotechnol.* **2015**, *90* (9), 1631–1639.
- (19) Feng, Y.; Meier, D. Extraction of Value-Added Chemicals from Pyrolysis Liquids with Supercritical Carbon Dioxide. *J. Anal. Appl. Pyrolysis* **2015**, *113*, 174–185.
- (20) Knez Hrnčič, M. K.; Venderbosch, R. H.; Škerget, M.; Knez, Z. Observation of Phase Behavior for Bio-Oil + Diesel + Carbon Dioxide and Bio-Oil + Tail Water + Carbon Dioxide System. *J. Chem. Eng. Data* **2013**, *58* (3), 648–652.
- (21) Hrnčič, M. K.; Venderbosch, R. H.; Škerget, M.; Ilic, L.; Knez, Z. Phase Equilibrium Data of Hydrogen in Pyrolysis Oil and Hydrogenated Pyrolysis Oil at Elevated Pressures. *J. Supercrit. Fluids* **2013**, *80*, 86–89.
- (22) Dahmen, N.; Abeln, J.; Eberhard, M.; Kolb, T.; Leibold, H.; Sauer, J.; Stapf, D.; Zimmerlin, B. The Bioliq Process for Producing Synthetic Transportation Fuels. *Wiley Interdiscip. Rev. Energy Environ.* **2017**, *6* (3), No. e236.
- (23) Pfitzer, C.; Dahmen, N.; Troger, N.; Weirich, F.; Sauer, J.; Gunther, A.; Muller-Hagedorn, M. Fast Pyrolysis of Wheat Straw in the Bioliq Pilot Plant. *Energy Fuels* **2016**, *30*, 8047–8054.
- (24) Riazi, M. R. A New Method for Experimental Measurement of Diffusion Coefficients in Reservoir Fluids. *J. Pet. Sci. Eng.* **1996**, *14*, 235–250.
- (25) Christov, M.; Dohrn, R. High-Pressure Fluid Phase Equilibria: Experimental Methods and Systems Investigated (1994–1999). *Fluid Phase Equilib.* **2002**, *202* (1), 153–218.
- (26) Etminan, S. R.; Maini, B. B.; Chen, Z.; Hassanzadeh, H. Constant-Pressure Technique for Gas Diffusivity and Solubility Measurements in Heavy Oil and Bitumen. *Energy Fuels* **2010**, *24* (1), 533–549.
- (27) Upreti, S. R.; Mehrotra, A. K. Experimental Measurement of Gas Diffusivity in Bitumen: Results for Carbon Dioxide. *Ind. Eng. Chem. Res.* **2000**, *39* (4), 1080–1087.
- (28) Surana, R. K.; Danner, R. P.; De Haan, A. B.; Beckers, N. New Technique to Measure High-Pressure and High-Temperature Polymer-Solvent Vapor-Liquid Equilibrium. *Fluid Phase Equilib.* **1997**, *139* (1–2), 361–370.
- (29) Span, R.; Wagner, W. A New Equation of State for Carbon Dioxide Covering the Fluid Region from the Triple-Point Temperature to 1100 K at Pressures up to 800 MPa. *J. Phys. Chem. Ref. Data* **1996**, *25* (6), 1509–1596.
- (30) Soave, G. S. Extension of the Classical Mixing Rules of the Redlich-Kwong Equation of State. *Chem. Eng. Sci.* **1972**, *27*, 1197–1203.
- (31) Kontogeorgis, G. M.; Michelsen, M. L.; Folas, G. K.; Derawi, S.; Von Solms, N.; Stenby, E. H. Ten Years with the CPA (Cubic-Plus-Association) Equation of State. *Part 1. Pure Compounds and Self-Associating Systems. Ind. Eng. Chem. Res.* **2006**, *45* (14), 4855–4868.
- (32) Michelsen, M. L.; Mollerup, J. M. *Thermodynamic Models: Fundamentals & Computational Aspects*, 2nd ed.; Tie-Line Publications, 2007.
- (33) AspenTech. <https://www.aspentech.com/en/products/engineering/aspen-hysys> (accessed Jun 2, 2021).

- (34) Briones, J. A.; Mullins, J. C.; Thies, M. C.; Kim, B. U. Ternary Phase Equilibria for Acetic Acid-Water Mixtures with Supercritical Carbon Dioxide. *Fluid Phase Equilib.* **1987**, *36*, 235–246.
- (35) Bamberger, A.; Sieder, G.; Maurer, G. High-Pressure (Vapor + Liquid) Equilibrium in Binary Mixtures of (Carbon Dioxide + Water or Acetic Acid) at Temperatures from 313 to 353 K. *J. Supercrit. Fluids* **2000**, *17*, 97–110.
- (36) Lucile, F.; Serin, J.-P.; Cézac, P.; Contamine, F.; Houssin, D.; Arpentinier, P. Solubility of Carbon Dioxide in Water and Aqueous Solution Containing Sodium Hydroxide at Temperatures from (293.15 to 393.15) K and Pressure up to 5 MPa: Experimental Measurements. *J. Chem. Eng. Data* **2012**, *57*, 784–789.
- (37) Yun, Z.; M. R. Shi, J. S. High Pressure Vapor-Liquid Phase Equilibrium for Carbon Dioxide-n-Butanol and Carbon Dioxide-i-Butanol. *Ranliao Huaxue Xuebao/Journal Fuel Chem. Technol.* **1996**, *24*, 87–92.
- (38) Lim, J. S.; Yoon, C. H.; Yoo, K. P. High-Pressure Vapor-Liquid Equilibrium Measurement for the Binary Mixtures of Carbon Dioxide +n-Butanol. *Korean J. Chem. Eng.* **2009**, *26* (6), 1754–1758.
- (39) Kariznovi, M.; Nourozieh, H.; Abedi, J. Solubility of Carbon Dioxide, Methane, and Ethane in 1-Butanol and Saturated Liquid Densities and Viscosities. *J. Chem. Thermodyn.* **2013**, *67*, 227–233.
- (40) Zúñiga-Moreno, A.; Galicia-Luna, L. A.; Sandler, S. I. Measurements of Compressed Liquid Densities for CO₂ (1) + Butan-1-ol (2) via a Vibrating Tube Densimeter at Temperatures from (313 to 363) K and Pressures up to 25 MPa. *J. Chem. Eng. Data* **2007**, *52* (5), 1960–1969.
- (41) Oasmaa, A.; Czernik, S. Fuel Oil Quality of Biomass Pyrolysis Oils - State of the Art for the End Users. *Energy Fuels* **1999**, *13* (4), 914–921.
- (42) Oasmaa, A.; Fonts, I.; Pelaez-Samaniego, M. R.; Garcia-Perez, M. E.; Garcia-Perez, M. Pyrolysis Oil Multiphase Behavior and Phase Stability: A Review. *Energy Fuels* **2016**, *30* (8), 6179–6200.
- (43) Oasmaa, A.; Kuoppala, E.; Solantausta, Y. Fast Pyrolysis of Forestry Residue. 2. Physicochemical Composition of Product Liquid. *Energy and Fuels* **2003**, *17*, 433–443.
- (44) Bridgwater, A. V.; Czernik, S.; Piskorz, J. An Overview of Fast Pyrolysis. In *Progress in Thermochemical Biomass Conversion*; Blackwell Science: Oxford, 2001; pp 977–997.
- (45) Fonts, I.; Atienza-Martínez, M.; Carstensen, H.-H.; Benés, M.; Pinheiro Pires, A. P.; Garcia-Perez, M.; Bilbao, R. Thermodynamic and Physical Property Estimation of Compounds Derived from the Fast Pyrolysis of Lignocellulosic Materials. *Energy Fuels* **2021**, *35*, 17114.
- (46) Ille, Y.; Sánchez, F. A.; Dahmen, N.; Pereda, S. Multiphase Equilibria Modeling of Fast Pyrolysis Bio-Oils. *Group Contribution Associating Equation of State Extension to Lignin Monomers and Derivatives*. *Ind. Eng. Chem. Res.* **2019**, *58* (17), 7318–7331.
- (47) Li, B.; Liu, G.; Xing, X.; Chen, L.; Lu, X.; Teng, H.; Wang, J. Molecular Dynamics Simulation of CO₂ Dissolution in Heavy Oil Resin-Asphaltene. *J. CO₂ Util.* **2019**, *33*, 303–310.
- (48) Zhou, J. H.; Zhu, R. X.; Zhou, J. M.; Chen, M. B. Molecular Dynamics Simulation of Diffusion of Gases in Pure and Silica-Filled Poly(1-Trimethylsilyl-1-Propyne) [PTMSP]. *Polymer (Guildf)*. **2006**, *47* (14), 5206–5212.
- (49) Carvalho, P. J.; Kurnia, K. A.; Coutinho, J. A. P. Dispelling Some Myths about the CO₂ Solubility in Ionic Liquids. *Phys. Chem. Chem. Phys.* **2016**, *18* (22), 14757–14771.
- (50) Klähn, M.; Seduraman, A. What Determines CO₂ Solubility in Ionic Liquids? A Molecular Simulation Study. *J. Phys. Chem. B* **2015**, *119* (31), 10066–10078.
- (51) Corvo, M. C.; Sardinha, J.; Casimiro, T.; Marin, G.; Seferin, M.; Einloft, S.; Menezes, S. C.; Dupont, J.; Cabrita, E. J. A Rational Approach to CO₂ Capture by Imidazolium Ionic Liquids: Tuning CO₂ Solubility by Cation Alkyl Branching. *ChemSusChem* **2015**, *8* (11), 1935–1946.
- (52) Seki, T.; Grunwaldt, J. D.; Baiker, A. In Situ Attenuated Total Reflection Infrared Spectroscopy of Imidazolium-Based Room-Temperature Ionic Liquids under “Supercritical” CO₂. *J. Phys. Chem. B* **2009**, *113* (1), 114–122.
- (53) Thran, A.; Kroll, C.; Faupel, F. Correlation between Fractional Free Volume and Diffusivity of Gas Molecules in Glassy Polymers. *J. Polym. Sci., Part B: Polym. Phys.* **1999**, *37* (23), 3344–3358.
- (54) Rindfleisch, F.; DiNoia, T. P.; McHugh, M. A. Solubility of Polymers and Copolymers in Supercritical CO₂. *J. Phys. Chem.* **1996**, *100* (38), 15581–15587.
- (55) Golzar, K.; Amjad-Iranagh, S.; Amani, M.; Modarress, H. Molecular Simulation Study of Penetrant Gas Transport Properties into the Pure and Nanosized Silica Particles Filled Polysulfone Membranes. *J. Membr. Sci.* **2014**, *451*, 117–134.
- (56) Wang, X. Y.; Raharjo, R. D.; Lee, H. J.; Lu, Y.; Freeman, B. D.; Sanchez, I. C. Molecular Simulation and Experimental Study of Substituted Polyacetylenes: Fractional Free Volume, Cavity Size Distributions and Diffusion Coefficients. *J. Phys. Chem. B* **2006**, *110* (25), 12666–12672.
- (57) Gwinner, B.; Roizard, D.; Lopicque, F.; Favre, E.; Cadours, R.; Boucot, P.; Carrette, P. L. CO₂ Capture in Flue Gas: Semiempirical Approach to Select a Potential Physical Solvent. *Ind. Eng. Chem. Res.* **2006**, *45* (14), 5044–5049.
- (58) Jonasson, A.; Persson, O.; Rasmussen, P.; Soave, G. S. Vapor-Liquid Equilibria of Systems Containing Acetic Acid and Gaseous Components. Measurements and Calculations by a Cubic Equation of State. *Fluid Phase Equilib.* **1998**, *152*, 67–94.
- (59) Kazarian, S. G.; Vincent, M. F.; Bright, F. V.; Liotta, C. L.; Eckert, C. A. Specific Intermolecular Interaction of Carbon Dioxide with Polymers. *J. Am. Chem. Soc.* **1996**, *118* (7), 1729–1736.
- (60) Li, M.; Zhang, J.; Zou, Y.; Wang, F.; Chen, B.; Guan, L.; Wu, Y. Models for the Solubility Calculation of a CO₂/Polymer System: A Review. *Mater. Today Commun.* **2020**, *25*, 101277.